Magnetic-Field Tuning of Hydrogen Bond Order-Disorder Transition in Metal-Organic Frameworks

Yinina Ma,[1,2] Yuxia Wang,[3] Junzhuang Cong,[1] and Young Sun[1,2,4,5,*]

[1]Beijing National Laboratory for Condensed Matter Physics and Beijing Advanced Innovation Center for Materials Genome Engineering, Institute of Physics, Chinese Academy of Sciences, Beijing 100190, China

[2]School of Physical Sciences, University of Chinese Academy of Sciences, Beijing 100190, China

[3]Department of Chemistry, State Key Laboratory of Elemento-Organic Chemistry, Nankai University, Tianjin 300071, China

[4]Songshan Lake Materials Laboratory, Dongguan, Guangdong 523808, China

[5]Beijing Academy of Quantum Information Sciences, Beijing 100193, China

(Received 16 February 2019; revised manuscript received 3 May 2019; published 25 June 2019)

The ordering of polar hydrogen bonds may break space inversion symmetry and induce ferroelectricity or antiferroelectricity. This process is usually immune to external magnetic fields so that magnetic control of hydrogen bonds is very challenging. Here we demonstrate that the ordering of hydrogen bonds in the metal-organic frameworks $[(CH_3)_2NH_2]M(HCOO)_3$ ($M = $ Fe, Co) can be manipulated by applying magnetic fields. After cooling in a high magnetic field, the order-disorder transition of hydrogen bonds shifts to a lower or higher temperature, depending on antiferroelectricity or ferroelectricity induced by hydrogen bond ordering. Besides, the order-disorder transition leads to a giant thermal expansion, exceeding $\sim 3.5 \times 10^4$ and $\sim 2 \times 10^4$ ppm for $M = $ Fe and Co, respectively, which is much higher than that of inorganic ferroelectrics. The influence of magnetic field on hydrogen bond ordering is discussed in terms of the magnetoelastic coupling.

DOI: 10.1103/PhysRevLett.122.255701

Hybrid inorganic-organic materials may exhibit unusual properties that are absent in classical inorganic and organic materials because they could combine both merits of inorganic and organic elements within a single phase [1,2]. As a prototype of hybrid materials, metal-organic frameworks (MOFs) consisting of networks of metal ions connected by coordinating organic linkers have been intensively studied in the past decade because of their diverse physical and chemical properties as well as the great potential in many applications [3–12].

The MOFs with the ABX_3 perovskite-like structure are of special interest because the variable A and B components provide plenty of room for adjusting the physical and chemical properties in a simple crystalline structure. In the last decade, many interesting magnetic and electric properties have been discovered in perovskite MOFs, including magnetic ordering [13,14], ferroelectric, and antiferroelectric ordering [15,16], multiferroicity [17,18], magnetoelectric coupling [19–23], resonant quantum magnetoelectric effect [24], large pyroelectric and thermal expansion coefficients [25,26], and so on.

In the ABX_3 perovskite MOFs, the organic cations occupying the A site form hydrogen bonds with the organic linkers X in order to be stabilized in the framework. The ferroelectricity or antiferroelectricity in them is mainly ascribed to the ordering of hydrogen bonds, though a hybrid nature of ferroelectricity involving both A and B sites was also proposed [27]. The order-disorder transition temperature of hydrogen bonds is determined by the competition between thermal fluctuation and bond energy, which is usually immune to external magnetic fields. As a consequence, magnetic field control of hydrogen bond ordering is very challenging and no success has been reported so far within our knowledge. In this work, we demonstrate that the order-disorder transition of hydrogen bonds in some perovskite MOFs can be actually manipulated by external magnetic fields.

The perovskite MOFs in this study have a formula of $[(CH_3)_2NH_2]M(HCOO)_3$ ($M = $ Fe, Co), termed as Fe-MOF and Co-MOF, respectively. The amine hydrogen atoms of the dimethylammonium (DMA^+) cations form hydrogen bonds with the oxygen atoms of the formate groups ($N-H\cdots O$). Single crystals of the MOFs were synthesized by the hydrothermal method. First, the solution containing 5 mmol $FeCl_2 \cdot 4H_2O$ or $CoCl_2 \cdot 6H_2O$, equal volume of deionized water and dimethylformamide (DMF) of 60 ml, is put in a 100 ml polytetrafluoroethylene-lined hydrothermal synthesis reactor, heating for 3 days at 140 °C. Then the supernatant was moved to a round-bottom flask for crystallization by slow evaporation at room temperature for 1 week. Finally, we removed the crystals from the mother liquid, washed them with ethanol for 3 times, and then stored them in Ar atmosphere. Powder x-ray diffraction (XRD) patterns at room temperature confirm the structure and phase purity of the synthesized perovskite MOFs. The single-crystal XRD patterns at room temperature shown

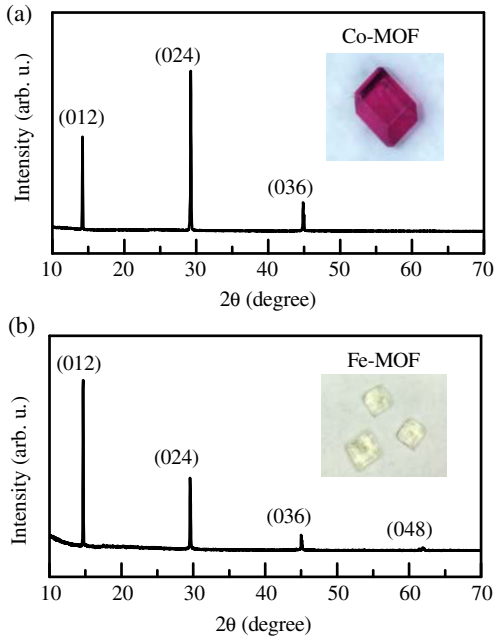

FIG. 1. The single-crystal XRD patterns at room temperature for (a) the Co-MOF and (b) the Fe-MOF. The insets show the images of the synthesized crystals.

in Figs. 1(a) and 1(b) suggest that the crystals of both MOFs are naturally grown layer by layer along the [012] direction. The size of the Fe-MOF and Co-MOF samples used in this work is $2.5 \times 2.5 \times 1.14$ mm^3 and $1.5 \times 1.3 \times 0.9$ mm^3, respectively, with the thin direction along the [012] direction.

Single-crystal XRD data of the Fe-MOF at 120 K were collected on an Agilent Supernova diffractometer using graphite monochromatic Mo $K\alpha$ radiation ($\lambda = 0.71073$ Å). The structure solution was performed by direct methods and further refinement was done by the full-matrix least-squares technique on F^2 with anisotropic thermal parameters for all nonhydrogen atoms using with the SHELXL program. Hydrogen atoms were located geometrically and refined isotropically.

The dielectric permittivity was measured by an Agilent 4980 LCR meter at a frequency of 1 kHz in a Cryogen-free Superconducting Magnet System (Oxford Instruments, TeslatronPT) with a homemade probe. For the pyroelectric measurements, the Co-MOF was poled in an electric field of 10 kV/cm from 200 to 5 K, and the Fe-MOF was cooled down from 180 to 110 K with a poling electric field of 6.6 kV/cm. After removing the poling electric field and releasing space charges for at least 30 min, the pyroelectric current was recorded with warming at a constant rate of 1 K/min. All the electric measurements were performed along the [012] direction of single-crystal samples. Thermal expansion was measured with a homemade capacitance dilatometer shown in Fig. 3(a). The change of sample length causes the shift of upper capacitor plate and subsequently induces a change in the capacitance [28]. The capacitance is precisely measured with an Andeen Hagerling 2700A capacitance bridge.

The ordering of hydrogen bonds ($N-H\cdots O$) introduces antiferroelectric (AFE) and ferroelectric (FE) order in the Fe-MOF and Co-MOF, respectively [17,29,30]. At room temperature, both the Fe-MOF and Co-MOF have the same structure, belonging to trigonal space group R-3c. After hydrogen bonds ordering, the low temperature structure of the Fe-MOF can be reasonably solved in monoclinic space group $C2/c$, keeping centrosymmetric. As shown in Fig. 2(a), the antiparallel arrangement of the DMA^+ cations along the b axis among nearest-neighbor chains leads to the essentially AFE order. The details of structural information for the Fe-MOF at room temperature and low temperature are summarized in Tables S1 and S2 in the Supplemental Material [31]. In contrast, as mentioned in Ref. [30], the hydrogen bonds of the Co-MOF are frozen in part at 93 K, rotating about a twofold axis [Fig. 2(b)].

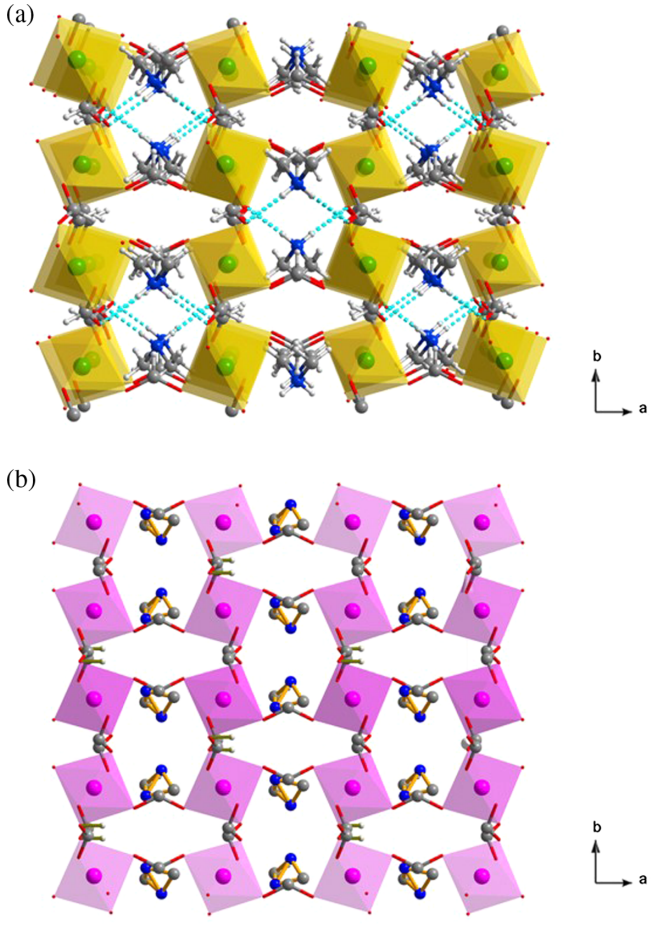

FIG. 2. (a) The crystal structure in the AFE phase of the Fe-MOF with centrosymmetric space group $C2/c$. The ordering hydrogen bonds among the nearest-neighbor chains arrange in antiparallel, which makes the polarization of neighbor chains offset. (b) The crystal structure in the FE phase of the Co-MOF with non-centrosymmetric space group Cc. The hydrogen bonds are frozen in part, rotating around a twofold axis.

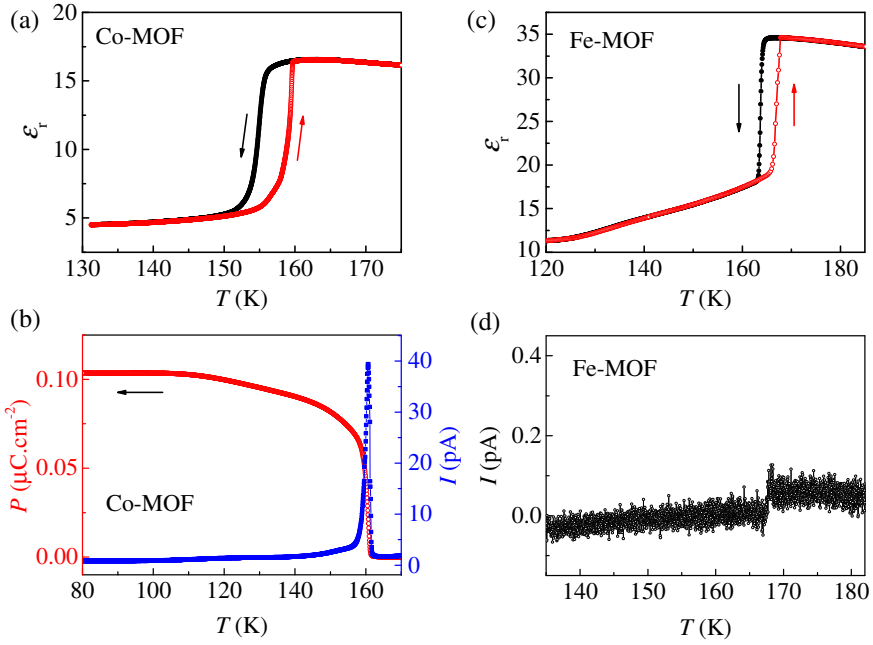

FIG. 3. Temperature dependence of dielectric permitivity for (a) the Co-MOF and (c) the Fe-MOF. (b) Pyroelectric current I and electric polarization P as a function of temperature for the Co-MOF. (d) Pyroelectric current I as a function of temperature for the Fe-MOF. These results further evidence that the ordering of hydrogen bonds induces the FE state in the Co-MOF and the AFE state in the Fe-MOF, respectively.

The partly ordering hydrogen bonds make the crystal structure down to noncentrosymmetric space group Cc, which belongs to 10 ferroelectric polar point groups.

The dielectric and pyroelectric properties further confirm the AFE and FE order in the Fe-MOF and Co-MOF, respectively. As shown in Figs. 3(a) and 3(c), the sudden jump in dielectric permittivity with a clear hysteresis signifies a first-order phase transition induced by the hydrogen bond ordering. In order to determine the nature of the low temperature phase, we measured the pyroelectric current as a function of temperature. As seen in Fig. 3(b), a pronounced pyroelectric peak appears at the phase transition temperature $T_C \sim 160$ K for the Co-MOF, which yields a relatively large electric polarization ($P \sim 0.1\ \mu\mathrm{C/cm^2}$). In contrast, as shown in Fig. 2(d), there is no clear pyroelectric peak at the phase transition for the Fe-MOF and thus the electric polarization is nearly zero.

The order-disorder transition of hydrogen bonds usually leads to a structural change. We employ a high-resolution capacitance dilatometer to detect the structural change associated with the order-disorder process of hydrogen bonds. Figure 4(a) illustrates the principle of the capacitance dilatometer in which a small variation in sample length is transformed into a change in the capacitance.

Figures 4(b) and 4(c) show the linear thermal expansion along the [012] direction for the ferroelectric Co-MOF and the antiferroelectric Fe-MOF, respectively. For both MOFs, there is a large lattice expansion along the [012] direction around T_C. The relative length change $\Delta L/L$ across this order-disorder phase transition reaches ~20 000 ppm for the Co-MOF and 35 000 ppm for the Fe-MOF, much higher than that of many inorganic ferroelectrics [32–34]. For instance, the maximum length change along the [001] direction across the ferroelectric phase transition in a $Pb(Mg_{1/3}Nb_{2/3})O_3 - 0.32PbTiO_3$(PMN − 0.32PT) single crystal is about 2600 ppm [32].

The giant thermal expansion associated with hydrogen bond order-disorder transition reflects the highly stretchable lattice of perovskite MOFs. When the hydrogen bonds are thermally ordered at low temperatures, the DMA^+ cations occupying the cavities in the ABX_3 perovskite structure are fixed by hydrogen bonding. As a consequence, the framework is strongly distorted by the interaction. At elevated temperatures, the DMA^+ cations become dynamically movable around a threefold axis in the cavities, which would release the distortion and drive the framework to expand.

The order-disorder process of hydrogen bonds is usually unaffected by magnetic fields. However, we find that this is not true for the perovskite MOFs studied here. When a magnetic field is applied along the [012] direction during the cooling process, the order-disorder transition of hydrogen bonds is apparently influenced. For the ferroelectric Co-MOF, the order-disorder transition of hydrogen bonds shifts to a higher temperature. As shown in Fig. 4(b), for a 10 T magnetic field, the temperature shift is ~0.9 K. This surprising result implies that an external magnetic field is in favor of the ordering of hydrogen bonds so that a higher thermal energy is required to drive the order-disorder transition. In strong contrast, for the antiferroelectric

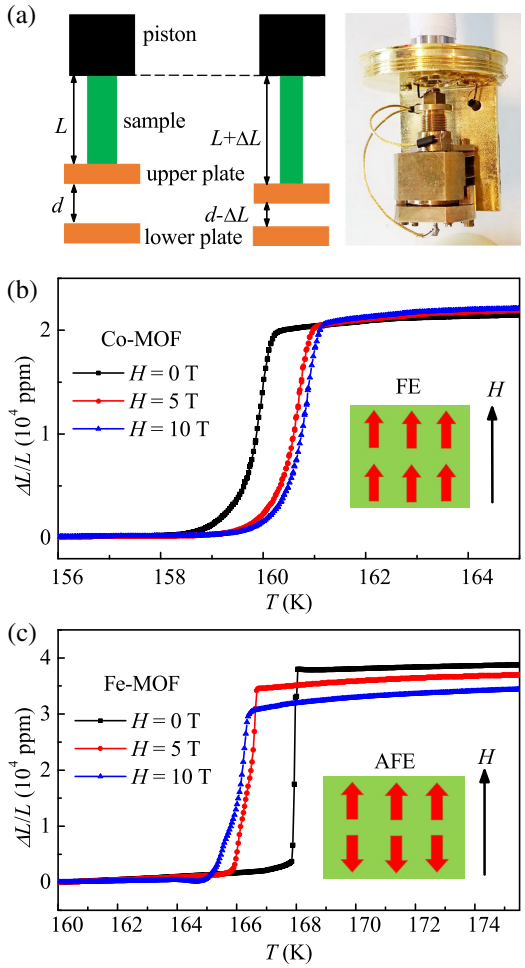

FIG. 4. (a) Schematic of a capacitance dilatometer. The linear expansion-striction of the sample is transformed into a change in the capacitance that is precisely measured by a capacitance bridge. Temperature dependence of the linear thermal expansion along the [012] direction in several magnetic fields for (b) the ferroelectric Co-MOF and (c) the antiferroelectric Fe-MOF. The order-disorder transition of hydrogen bonds causes a large change in length for both MOFs. After cooling in a high magnetic field, the transition temperature shifts to a higher temperatur for the Co-MOF but to a lower temperature for the Fe-MOF.

Fe-MOF, the transition temperature shifts to a lower temperature after cooling in a high magnetic field, as shown in Fig. 4(c). For a 10 T magnetic field, the temperature shift is ~2 K. It indicates that a high magnetic field is able to destabilize the ordering of hydrogen bonds so that they become thermally disordered at a lower temperature. The shift of phase transition in response to applied magnetic field is further confirmed by the temperature dependence of dielectric permitivity measured in a high magnetic field, shown in Fig. S1 in Supplemental Material [31]. After cooling in 10 T, the dielectric phase transition shifts to a higher temperature for the Co-MOF, but to a lower temperature for the Fe-MOF, qualitatively consistent with the thermal expansion data.

The completely different behaviors in response to external magnetic fields between the Co-MOF and Fe-MOF are very interesting. Both MOFs have a similar perovskite structure and the same type of hydrogen bonds ($N-H\cdots O$). The major difference between them is that the ordering of hydrogen bonds induces the FE state in the Co-MOF but the AFE state in the Fe-MOF. The polar hydrogen bonds would be oriented antiparallel in the AFE state and parallel in the FE state, as schematically illustrated in the insets of Figs. 4(b) and 4(c), respectively.

Based on our experimental results, it is concluded that the role of applied magnetic fields during the cooling process is to help align polar hydrogen bonds in a parallel way. In this case, the FE state with the collectively parallel ordering of hydrogen bonds becomes more stable under a high magnetic field. Thus, a higher thermal energy is required to destroy the ordering. Consequently, the order-disorder transition shifts to a higher temperature. By contrast, in the AFE state, the polar hydrogen bonds tend to orient antiparallel, which is against the role of external magnetic fields. Under a high magnetic field, the antiparallel ordering of hydrogen bonds becomes less stable near the phase transition so that lower thermal fluctuations are able to destroy the ordering. As a result, the order-disorder transition starts at a lower temperature.

In general, external magnetic fields align partially the magnetic moments of magnetic Fe^{2+} or Co^{2+} ions and cause a small striction or expansion along the applied magnetic field (the magnetoelastic effect). There has been some evidence for the magnetoelastic coupling even in the paramagnetic state in the MOFs [19,34–37]. The local magnetoelastic coupling probably induces a small lattice change under a high magnetic field, which would make the M-O_6 octahedron distorted slightly. Recent studies imply that the framework distortion is also a significant element in the ordering of the DMA^+ cation [38]. For the Co-MOF, the Co cations are in a distorted octahedron environment with six different Co-O distances at the low temperature phase. High magnetic fields would further deform the octahedron, which may make the long Co-O bond weaker, thus allowing greater negative charge to reside on O. This behavior increases the intensity of $N-H\cdots O$ bonding. Moreover, the more distorted octahedron is likely to promote a parallel alignment of hydrogen bonds. These two changes both have a positive effect on strengthening the parallel ordering of hydrogen bonds. For the Fe-MOF, the deformed $Fe-O_6$ octahedron contains three groups of Fe-O bonds with different distance. This environment makes hydrogen bonds prefer an antiparallel arrangement. Applying a high magnetic field may further deform the octahedron and reduce the energy of antiparallel ordering of hydrogen bonds. The energy scale could be estimated from the temperature shift (~2 K) under a 10 T magnetic field, corresponding to ~0.1 meV. Although this magnetic field effect is not prominent at this stage, it strongly

indicates the potential of magnetic control of hydrogen bonds in hybrid inorganic-organic materials. We expect that this finding would stimulate more interest in this appealling topic.

In summary, the order-disorder transition of hydrogen bonds in the perovskite MOFs containing magnetic Fe^{2+} and Co^{2+} ions produces a giant thermal expansion, much higher than that of many inorganic ferroelectrics. Moreover, the ordering process of hydrogen bonds can be manipulated by applying magnetic fields due to the magnetoelastic coupling. As a consequence, the order-disorder transition shifts to a higher or lower temperature under a high magnetic field, depending on the FE or AFE state.

This work was supported by the National Natural Science Foundation of China (Grants No. 51725104 and No. 11534015), the National Key Research and Development Program of China (Grant No. 2016YFA0300701), Beijing Natural Science Foundation (Grant No. Z180009), and BAQIS Research Program (Grant No. Y18G10).

*Corresponding author.
youngsun@iphy.ac.cn

[1] C. N. R. Rao, A. K. Cheetham, and A. Thirumurugan, J. Phys. Condens. Matter **20**, 083202 (2008).
[2] W. Li, Z. Wang, F. Deschler, S. Gao, R. H. Friend, and A. K. Cheetham, Nat. Rev. Mater. **2**, 16099 (2017).
[3] W. Zhang and R. G. Xiong, Chem. Rev. **112**, 1163 (2012).
[4] P. Canepa, N. Nijem, Y. J. Chabal, and T. Thonhauser, Phys. Rev. Lett. **110**, 026102 (2013).
[5] C. Wang, D. Liu, and W. Lin, J. Am. Chem. Soc. **135**, 13222 (2013).
[6] Y. Tian, W. Wang, Y. Chai, J. Cong, S. Shen, L. Yan, S. Wang, X. Han, and Y. Sun, Phys. Rev. Lett. **112**, 017202 (2014).
[7] H. Babaei and C. E. Wilmer, Phys. Rev. Lett. **116**, 025902 (2016).
[8] B. Li, H. M. Wen, Y. Cui, W. Zhou, G. Qian, and B. Chen, Adv. Mater. **28**, 8819 (2016).
[9] M. G. Yamada, H. Fujita, and M. Oshikawa, Phys. Rev. Lett. **119**, 057202 (2017).
[10] M. R. Ryder, B. Van de Voorde, B. Civalleri, T. D. Bennett, S. Mukhopadhyay, G. Cinque, F. Fernandez-Alonso, D. De Vos, S. Rudić, and J.-C. Tan, Phys. Rev. Lett. **118**, 255502 (2017).
[11] J. Kundu, J. F. Stilck, J.-H. Lee, J. B. Neaton, D. Prendergast, and S. Whitelam, Phys. Rev. Lett. **121**, 015701 (2018).
[12] P. C. Rout and V. Srinivasan, Phys. Rev. Mater. **2**, 014407 (2018).
[13] X. Y. Wang, L. Gan, S. W. Zhang, and S. Gao, Inorg. Chem. **43**, 4615 (2004).
[14] D. F. Weng, Z. M. Wang, and S. Gao, Chem. Soc. Rev. **40**, 3157 (2011).
[15] P. Jain, N. S. Dalal, B. H. Toby, H. W. Kroto, and A. K. Cheetham, J. Am. Chem. Soc. **130**, 10450 (2008).
[16] F. R. Fan, H. Wu, D. Nabok, S. Hu, W. Ren, C. Draxl, and A. Stroppa, J. Am. Chem. Soc. **139**, 12883 (2017).
[17] P. Jain, V. Ramachandran, R. J. Clark, H. D. Zhou, B. H. Toby, N. S. Dalal, H. W. Kroto, and A. K. Cheetham, J. Am. Chem. Soc. **131**, 13625 (2009).
[18] D. Di Sante, A. Stroppa, P. Jain, and S. Picozzi, J. Am. Chem. Soc. **135**, 18126 (2013).
[19] W. Wang, L. Yan, J. Cong, Y. Zhao, F. Wang, S. Shen, T. Zou, D. Zhang, S. G. Wang, X. Han, and Y. Sun, Sci. Rep. **3**, 2024 (2013).
[20] Y. Tian, A. Stroppa, Y. Chai, L. Yan, S. Wang, P. Barone, S. Picozzi, and Y. Sun, Sci. Rep. **4**, 6062 (2014).
[21] Y. Tian, J. Cong, S. Shen, Y. Chai, L. Yan, S. Wang, and Y. Sun, Phys. Status Solidi RRL **8**, 91 (2014).
[22] L. C. Gómez-Aguirre, B. Pato-Doldán, J. Mira, S. Castro-García, M. A. Señarís-Rodríguez, M. Sánchez-Andújar, J. Singleton, and V. S. Zapf, J. Am. Chem. Soc. **138**, 1122 (2016).
[23] P. Jain, A. Stroppa, D. Nabok, A. Marino, A. Rubano, D. Paparo, M. Matsubara, H. Nakotte, M. Fiebig, S. Picozzi, E. S. Choi, A. K. Cheetham, C. Drax, N. S. Dalal, and V. S. Zapf, npj Quantum Mater. **1**, 16012 (2016).
[24] Y. Tian, S. Shen, J. Cong, L. Yan, S. Wang, and Y. Sun, J. Am. Chem. Soc. **138**, 782 (2016).
[25] M. Sánchez-Andújar, L. Gómez-Aguirre, B. P. Doldán, S. Yáñez-Vilar, R. Artiaga, A. Llamas-Saiz, R. Manna, F. Schnelle, M. Lang, and F. Ritter, CrystEngComm **16**, 3558 (2014).
[26] Y. Ma, J. Cong, Y. Chai, L. Yan, D. Shang, and Y. Sun, Appl. Phys. Lett. **111**, 042901 (2017).
[27] A. Stroppa, P. Barone, P. Jain, J. M. Perez-Mato, and S. Picozzi, Adv. Mater. **25**, 2284 (2013).
[28] R. Küchler, T. Bauer, M. Brando, and F. Steglich, Rev. Sci. Instrum. **83**, 095102 (2012).
[29] Y. Ruchika, D. Swain, H. L. Bhat, and E. Suja, J. Appl. Phys. **119**, 064103 (2016).
[30] D. W. Fu, W. Zhang, H. L. Cai, Y. Zhang, J. Z. Ge, R. G. Xiong, S. D. Huang, and N. Takayoshi, Angew. Chem., Int. Ed. Engl. **50**, 11947 (2011).
[31] See Supplemental Material at http://link.aps.org/supplemental/10.1103/PhysRevLett.122.255701 for the detailed structural information of the Fe-MOF, and the influence of magnetic field on dielectric permittivity.
[32] Z. Li, Z. Xu, Z. Xi, F. Xiang, and X. Yao, Ferroelectrics **355**, 245 (2007).
[33] P. Hu, J. Chen, J. Deng, and X. Xing, J. Am. Chem. Soc. **132**, 1925 (2010).
[34] M. V. Gorev, I. N. Flerov, Ph. Sciau, and S. Guillemet-Fritsch, Phys. Solid State **51**, 790 (2009).
[35] R. I. Thomson, P. Jain, A. K. Cheetham, and M. A. Carpenter, Phys. Rev. B **86**, 214304 (2012).
[36] L. Xin, Z. Zhang, M. A. Carpenter, M. Zhang, F. Jin, Q. Zhang, X. Wang, W. Tang, and X. Lou, Adv. Funct. Mater. **28**, 1806013 (2018).
[37] K. Vinod, C. S. Deepak, Shilpam Sharma, D. Sornadurai, C. S. Sundar, and A. Bharathi, RSC Adv. **5**, 37818 (2015).
[38] H. D. Duncan, M. T. Dove, D. A. Keen, and A. E. Phillips, Dalton Trans. **45**, 4380 (2016).